Journal of Photochemistry and Photobiology A: Chemistry 154 (2002) 33–39

Journal of Photochemistry and Photobiology A:Chemistry

www.elsevier.com/locate/jphotochem

Excited-state intramolecular proton transfer in photochromic jet-cooled *N*-salicylideneaniline

Nobuto Otsubo [a,b], Chie Okabe [a,b], Hirotoshi Mori [a,b], Kenji Sakota [a,b],
Kiichi Amimoto [c,d], Toshio Kawato [c,d], Hiroshi Sekiya [a,b,*]

[a] *Department of Chemistry, Faculty of Sciences, Kyushu University, 6-10-1 Hakozaki, Higashi-ku, Fukuoka 812-8581, Japan*
[b] *Department of Molecular Chemistry, Graduate School of Science, Kyushu University, 6-10-1 Hakozaki, Higashi-ku, Fukuoka 812-8581, Japan*
[c] *Department of Chemistry, Faculty of Sciences, Kyushu University, 4-2-1 Ropponmatsu, Chuo-ku, Fukuoka 810-8560, Japan*
[d] *Department of Molecular Chemistry, Graduate School of Science, Kyushu University, 4-2-1 Ropponmatsu, Chuo-ku, Fukuoka 810-8560, Japan*

Received 4 March 2002; received in revised form 16 May 2002; accepted 28 May 2002

Abstract

The laser induced fluorescence (LIF) and dispersed fluorescence spectra of jet-cooled *N*-salicylideneaniline have been observed in a supersonic free jet for the first time. The spectrum shows a very broad feature with no vibronic structure in the 24,800–28,800 cm^{-1} region except for a broad peak at 28,200 cm^{-1}. The broad feature of the spectrum has been ascribed to the homogeneous broadening of vibronic bands due to very fast internal conversion from the $^1(\pi\pi^*)$ to $^1(n\pi^*)$ state which is located below the $^1(\pi\pi^*)$ state as well as to the excited-state intramolecular proton transfer (ESIPT) reaction. No resonance emission has been detected following the excitation of the $^1(\pi\pi^*)$ state of the enol form, while anomaly Stokes-shifted fluorescence was observed at 15,000–20,500 cm^{-1}. The dispersed fluorescence spectra show two broad maxima separated by 700–1000 cm^{-1}, suggesting that two keto tautomers are produced via the ESIPT reaction. The existence of the corresponding two *cis*-keto tautomers with similar energies has been suggested by density functional theory (DFT) calculations at the B3LYP/6-31G** level and ab initio calculations at the HF/6-31G** level.
Published by Elsevier Science B.V.

Keywords: *N*-Salicylideneaniline; Proton transfer; Photochromism; Electronic spectrum; Supersonic jet; Internal conversion

1. Introduction

The photochromism of *N*-salicylideneaniline (SA) has been of considerable interests in its properties and application. The photochromic reaction of SA has been extensively studied with various spectroscopic methods such as steady-state absorption and emission spectroscopy [1–5], time-resolved transient spectroscopy [4–8], time-resolved IR spectroscopy [9], and polarized reflection spectroscopy [10]. Photoexcitation of the enol form of SA (Fig. 1) with UV light prepares electronically excited sate followed by rapid excited-state intramolecular proton transfer (ESIPT), producing very long-lived transients [1–10]. Spectroscopic measurements together with theoretical calculations have provided information about the transition energies, ESIPT rate, and structures of the precursor of photochromic products. In spite of great efforts devoted to understanding the photochromism of SA, controversial results have been given for the precursor species of the photochromic intermediate transients and conformations of the ESIPT products. A difficulty in complete understanding of the photochromism arises from the existence of structural isomers for the keto form; number of the isomers depends on the literature [1–11].

Long-lived intermediate transient of SA has been ascribed to either a *trans*-keto form or a zwitterionic form. Harada et al. [12] identified a *trans*-keto form of a crystalline salicylideneaniline derivative generated by two-photon absorption of the enol form. This study clearly showed that the long-lived transient responsible for the photochromism in the crystalline state is a *trans*-keto tautomer. Time-resolved studies on SA in solution suggested that the fluorescent phototautomer and the photochromic transient have a common precursor, which is considered to be a hot vibrationally excited keto tautomer [6,8]. However, recent theoretical calculations predicted that common precursor of the fluorescent keto tautomer and photochromic transient is unstable planar $^1(\pi\pi^*)$ enol tautomer [11]. It has been believed that the fluorescent tautomer has a *cis*-keto form. However, we noticed that different energy level schemes have been proposed for the S_0 and S_1 state of the *cis*-keto form [1,6]. Two electronic ground states exist for the *cis*-keto form in a model of

---

[*] Corresponding author. Tel.: +81-92-642-2574; fax: +81-92-642-2607.
E-mail address: hsekiscc@mbox.nc.kyushu-u.ac.jp (H. Sekiya).

1010-6030/02/$ – see front matter. Published by Elsevier Science B.V.
PII: S1010-6030(02)00306-4

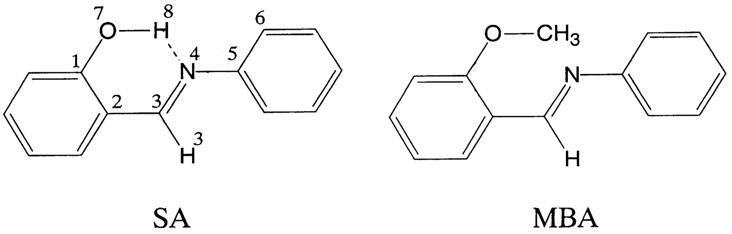

Fig. 1. Structures of the enol form of SA and MBA. The numbering of atoms in SA is used to designate structural parameters in Table 1.

Higelin and Sixl [1], whereas only a single state is proposed by Barbara et al. [6]. The determination of the conformation of the *cis*-keto form is important to understand the fluorescence channel, but the conformation of fluorescent *cis*-keto tautomer has not been clearly identified.

Semiempirical calculations [3,8], CIS/6-31G* and time-dependent density functional theory (TD/DFT) calculations [11] predicted that the $^1(n\pi^*)$ state lies close to the $^1(\pi\pi^*)$ state in the enol form. The relative energies of the two states depend on the torsional angle between the anilino ring and the phenol ring. Since the $^1(n\pi^*)$ state is located below the $^1(\pi\pi^*)$ state for nonplanar configuration, the interaction between the $^1(n\pi^*)$ and $^1(\pi\pi^*)$ states may substantially influence the excited-sate dynamics of SA, however, the $^1(n\pi^*)$ state has not been observed. In addition, the S_1–S_0 transition energy of the enol form has been obtained from very broad absorption spectrum measured in the condensed phase. The S_1–S_0 transition energy reported so far ranges from 26,000 to 31,000 cm^{-1} [1,3,5]. The determination of the S_1–S_0 $(\pi\pi^*)$ transition energy and observation of the $^1(\pi\pi^*)$ state are important to discuss the excited-state dynamics of SA.

The measurement of the electronic spectrum of SA under the isolated jet-cooled conditions is a powerful tool to investigate ESIPT reactions [13]. To our best of knowledge, no report has been presented about the electronic spectrum of SA in the isolated state. Thus, we have measured the fluorescence excitation and dispersed fluorescence spectra of jet-cooled SA. We had expected that sharp vibronic bands might appear in the excitation spectrum. Contrary to our expectations, the observed excitation spectrum is very broad, however, the spectrum involves valuable information on the excited-state potential and dynamics. We have carried out density functional theory (DFT) calculations for stable conformations in the ground state. We will discuss the origin of the broad feature of the excitation spectrum and stable conformations of keto tautomers associated with the fluorescence channel.

2. Experimental

SA and *N*-(2-methoxybenzylidene) aniline (MBA) (Fig. 1) used in this study were prepared by direct condensation of the appropriate aldehyde with aniline in methanol, followed by recrystallization from alcohol to yield the pure compounds suitable for measurement as yellow crystalline powder [14–16]. They were identified by satisfactory elemental analytical data and ^{1}H NMR and IR spectral data.

The UV and fluorescence spectra of SA and MBA in *n*-hexane solution were measured with UV-2500(PC)S (Shimadzu) and FP750 (JASCO) spectrometers, respectively.

The experimental apparatus for the laser induced fluorescence (LIF) excitation and dispersed fluorescence spectra in a supersonic jet was essentially the same as that reported previously [17,18]. SA was heated to 100–140 °C by a coiled heater. The vaporized SA molecules were mixed with helium carrier gas, and expanded into a vacuum chamber with a pulsed nozzle (general valve, $D = 0.5\,\mathrm{mm}$). The backing pressure of He was 3 atm. The SA molecules were excited with an excimer laser pumped dye laser system (Lumonics EX-600 and HD-300). Five laser dyes (Excition), E398, QUI, a mixture of QUI and BPBD365 (1:9), DMQ, and E351, were used to obtain wavelengths between 345 and 405 nm. The LIF spectrum was measured by monitoring total fluorescence with a photomultiplier (Hamamatsu 1P28A). We have attempted to detect long-lived intermediate transients produced from the ESIPT reaction by using a two-step laser excitation technique with two nanosecond laser systems. The third harmonics of a Nd:YAG laser (Spectra Physics 230) ($\lambda = 355\,\mathrm{nm}$) was used to excite the enol form of SA, while an excimer laser pumped dye laser system (Lumonics EX-600 and HD-300) was used to probe the keto form. The time delay between the two laser pulses was varied between 50 and 500 ns.

The dispersed fluorescence spectrum was measured with a monochromator (Spex 1704, $f = 0.85\,\mathrm{m}$) equipped with a photomultiplier (Hamamatsu R955). The electric current from the photomultiplier was fed into a digital oscilloscope (LeCroy 9310A) and the averaged signal was stored on a PC computer.

3. Results

3.1. Absorption and fluorescence spectra in solution

Fig. 2 shows the absorption and fluorescence spectra of SA and MBA in *n*-hexane solution at room temperature. The

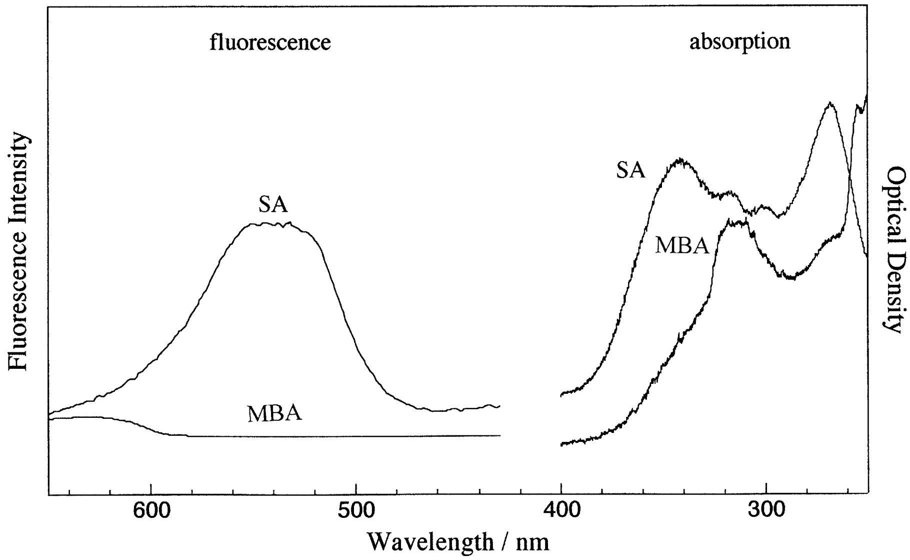

Fig. 2. Absorption spectra of SA and MBA in *n*-hexane solution (10^{-4} M) at room temperature. Fluorescence spectra of SA and MBA in *n*-hexane solution (10^{-6} M) at room temperature obtained by exciting in 345 and 315 nm, respectively. No fluorescence is detected from MBA, and a broad signal below 600 nm is due to scattered light used for excitation.

onset of absorption is ∼390 nm, and an absorption maximum is observed at 340 nm in the spectrum of SA. Previously, this maximum has been assigned to the electronic origin of the S_1–S_0 ($\pi\pi^*$) transition [1–8]. In addition to the peak at 340 nm, two unassigned shoulders and a peak are observed at 320, 305, and 270 nm, respectively. The absorption spectrum of MBA is similar to SA, while an absorption maximum of MBA (315 nm) is 25 nm blue-shifted with respect the corresponding peak of SA at 340 nm. The blue-shift of the absorption maximum of MBA must be due to the absence of the intramolecular hydrogen bond that stabilizes the excited-state energy.

It should be noticed that no resonance fluorescence is observed in the spectrum of MA as well as SA, although strongly Stokes-shifted broad emission is observed between 440 and 640 nm in the spectrum of SA. The emission must be due to the proton-transferred keto form of SA. The intensity of fluorescence from MBA is too weak to be detected. The fluorescence quantum yield of SA was determined to be 0.6×10^{-3} [3], and that of MBA may be more than two orders smaller than that of SA.

3.2. Fluorescence excitation and dispersed fluorescence spectra in the isolated state

Fig. 3 displays the fluorescence excitation spectrum of jet-cooled SA in the 24,800 and 28,800 cm^{-1} region. The intensity of fluorescence was corrected against the laser power. The LIF spectrum in Fig. 3 was obtained by connecting the spectrum of five wavelength regions through normalizing the intensity of fluorescence at the connected wavelengths. The LIF spectrum is very broad, and the intensity of fluorescence gradually increases with the excitation energy. No vibronic structure has been observed except for a broad peak at 28,200 cm^{-1}.

Mirta and Tamai [8] reported the observation of resonance fluorescence with a peak at 325 nm by exciting higher energy region of the S_1–S_0 transition of SA in solution. The resonance fluorescence was ascribed to the S_2–S_0 transition. We scanned the laser wavelength in the S_2–S_0 region (260–290 nm) of SA reported by Mitra and Tamai [8]. However, no vibronic bands due to SA have been observed.

Fig. 4a and b display the dispersed fluorescence spectrum of SA excited in 27,320 and 28,570 cm^{-1}, respectively. The fluorescence spectrum is anomaly Stokes-shifted with respect to the excitation energy, while no resonance emission has been observed. When the excitation was lowered to 25,000 cm^{-1} resonance fluorescence was absent, indicating that fluorescence is originating only from the proton transferred keto form. Two broad maxima separated by 700–1000 cm^{-1} are observed in the dispersed fluorescence spectra in Fig. 4. Doublet structure has been observed in the dispersed fluorescence spectra in stilbene and biphenyl host [1].

Long-lived transients following the excitation of the enol form were observed in acetonitrile solution [3] and in low temperature crystal and glass [1]. The long-lived transients are ascribed to nonhydrogen bonded *trans*-keto tautomer or the zwitterionic tautomer. Kownacki et al. [3] observed the S_1–S_0 excitation spectrum in the 14,000–19,000 cm^{-1} region due to long-lived transients in acetonitrile solution by using two-step LIF method with the delay time of the pump and excited pump pulses was 170 ns. We excited the enol form of SA with the third harmonics of the Nd:YAG laser (355 nm), and attempted to detect the long-lived transients by tuning the wavelength of the probe laser between 16,000 and 18,000 cm^{-1}. The delay time between the pump and

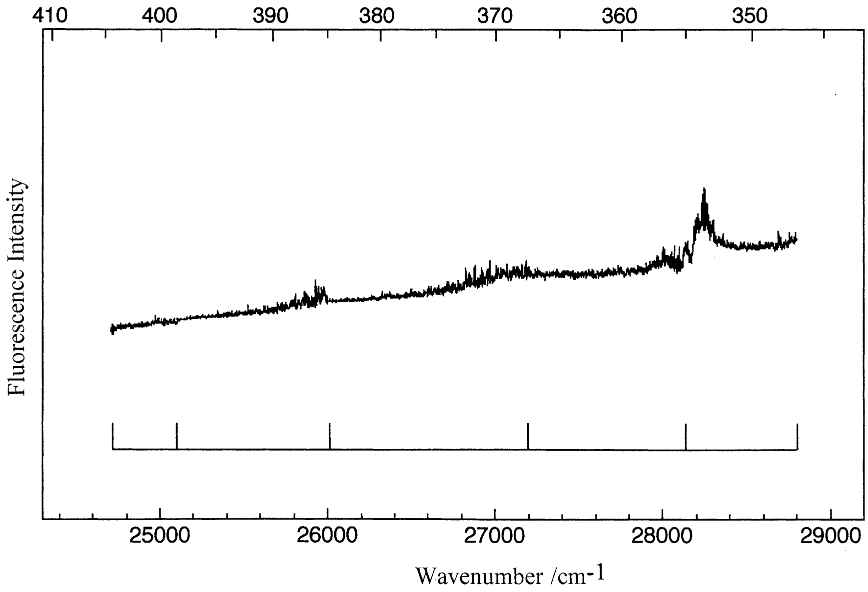

Fig. 3. LIF spectrum of jet-cooled SA by monitoring Stokes-shifted fluorescence with a cutoff filter (Toshiba Y-48). The intensity of fluorescence was corrected against the laser power and the spectra of five wavenumber regions were connected. The scale under the spectrum shows positions where LIF spectra are connected. The backing pressure of He was 3 atm. Only a broad band is observed at 28,200 cm^{-1}, and the other weak sharp peaks are due to noise generated by the correction of fluorescence signal against very weak laser intensity.

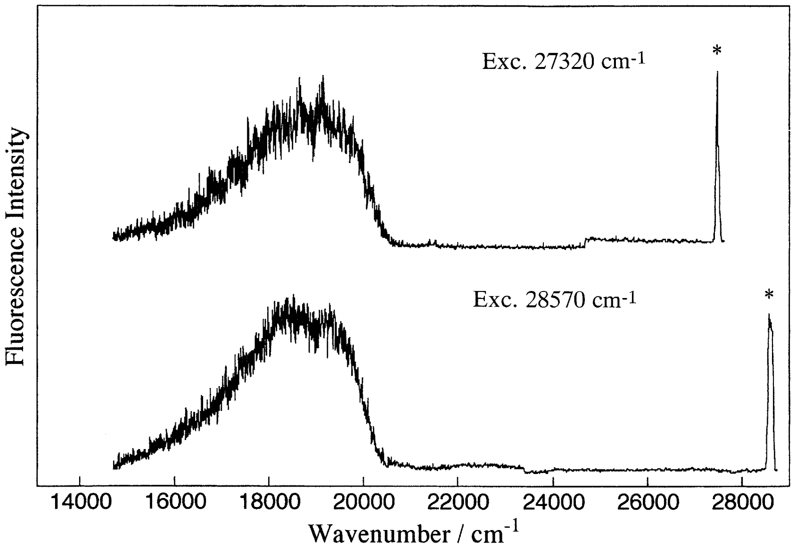

Fig. 4. Dispersed fluorescence spectra of SA excited in 27,320 and 28,570 cm^{-1}. The asterisk indicates the scattered laser light. The resolution of the spectrum is 60 cm^{-1}.

probe pulses was varied from 50 to 500 ns, however, no LIF signal was detected.

4. Discussion

4.1. Origin of broad feature in the LIF spectrum

The LIF spectrum of SA is very broad in the observed 24,800–28,800 cm^{-1} region. The excitation of the enol tautomer of SA in this region provides only Stokes-shifted fluorescence. Stable structures of the enol form of SA in the $^1(\pi\pi^*)$ and $^1(n\pi^*)$ states are planar and nonplanar, respectively [11]. The SA molecule in the S_0 state is nonplanar, but in the excited-state the molecule should be planar or nearly planar to undergo the ESIPT reaction [11,19]. The ESIPT reaction occurs for the excitation in the whole wavenumber region in Fig. 3, therefore, the LIF spectrum is ascribed to the S_1–S_0 $(\pi\pi^*)$ transition. The broad band at 28,200 cm^{-1} is located above about 3400 cm^{-1} from the onset of the LIF spectrum. There is a possibility that the band at 28,200 cm^{-1} is due to the OH stretching mode, since the OH bond length may significantly change upon photoexcitation. However, we cannot definitely give an unambiguous assignment for this band, because the electronic origin of the S_1–S_0 ($\pi\pi^*$) transition is not clear from the observed spectrum.

We had expected that sharp vibronic bands might appear in the fluorescence excitation spectrum. However, no sharp bands are observed in Fig. 3, and only a broad peak is observed at 28,200 cm^{-1}. The frequencies of the torsional mode in the S_0 state and S_1 ($\pi\pi^*$) state of the enol form are calculated to be 60 and 40 cm^{-1}, respectively [11]. The ESIPT rates have been determined to be $(210\,\mathrm{fs})^{-1}$ and $(380\,\mathrm{fs})^{-1}$ in cyclohexane and in ethanol solution, respectively, when the normal enol form of SA was excited at 360 nm [7,8]. The homogeneous line width of vibronic bands $\mathrm{fwhm_{homo}} = (2\pi c\tau)^{-1}$ in the fluorescence excitation spectrum is estimated to be 28 cm^{-1} by assuming an ESIPT rate (τ^{-1}) of $(210\,\mathrm{fs})^{-1}$ in cyclohexane solution. These considerations reflect that a rapid process exists in addition to the ESIPT reaction following the excitation of the S_1 ($\pi\pi^*$) state of the enol form, and overlapping of broad torsional vibrations may provide the very broad feature.

Possible nonradiative processes following the excitation of the S_1 ($\pi\pi^*$) state are internal conversion to the S_1 ($n\pi^*$) and S_0 states and intersystem crossing to the triplet state. The occurrence of rapid internal conversion from the S_1 ($\pi\pi^*$) to S_1 ($n\pi^*$) state has been suggested by theoretical calculations [11], but no experimental evidence has been obtained. Recent calculations at the HF/6-31G* level show that the SA molecule in the ground state is nonplanar and the anilino group is twisted by 44°, while the phenol ring and the C(3)–H(3)–N bridge remain in the same plane [11]. The calculated angle is close to the observed angle (49°) in crystal [20]. The TD/B3LYP excitation energies to the two lowest excited-states obtained at the HF/6-31G* geometry are 3.26 ($\pi\pi^*$) and 3.29 eV ($n\pi^*$). In the C_s symmetry the lowest singlet state is $^1(\pi\pi^*)$. The S_1 ($n\pi^*$) state stabilizes by a twist of the phenol ring which is almost perpendicular to the anilino ring. Since the S_1 ($n\pi^*$) state of the enol form of SA is located below the S_1 ($\pi\pi^*$) state, photoexcited SA may undergo rapid internal conversion upon the twist of the phenol ring. The broad spectral feature could be well explained by taking into account of rapid nonradiative processes including internal conversion from the S_1 ($\pi\pi^*$) to S_1 ($n\pi^*$) state that competes with the ESIPT reaction.

4.2. Structures of keto tautomer and two transition systems in the dispersed fluorescence spectrum and photoproducts

Stable structures of SA were optimized with the DFT calculations at the B3LYP/6-31G** level and ab initio calculations at the HF/6-31G** level by using a GAUSSIAN'98 and GAMESS program packages [21,22]. The optimized structures obtained with the B3LYP/6-31G** basis sets are illustrated in Fig. 5 and their structural parameters are listed in Table 1. Ab initio calculations at the HF/6-31G** level provided very similar structures as those obtained by DFT calculations. The relative energies of tautomers are listed in Table 2. Only one stable tautomer exists for the enol form, whereas four stable tautomers are obtained for the keto form. We refer the five tautomers as Enol, *cis*-keto I, *cis*-keto II, *cis*-keto III, and *trans*-keto. The conformations of Enol and *trans*-keto tautomers are essentially the same as those reported previously [11]. It should be noted that

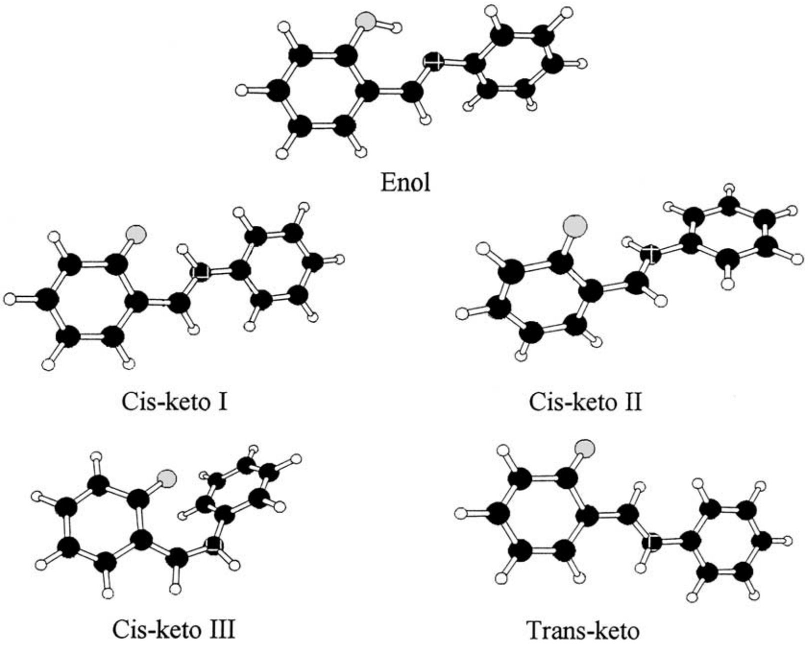

Fig. 5. Optimized structures for SA calculated at the B3LYP/6-31G** level.

Table 1
Structural parameters of SA in the ground state calculated at the B3LYP/6-31G** level[a]

		Enol	*Cis*-keto I	*Cis*-keto II	*Cis*-keto III	*Trans*-keto
Bond length (Å)	O(7)–H(8)	0.998	1.636	3.029		
	N(4)–H(8)	1.721	1.053	1.040		
	O(7)–N(4)	2.622	2.558	3.175		
Bond angle (°)	O(7)–H(8)–N(4)	148.1	143.2	88.4		
Dihedral angle	C(1)–C(2)–C(3)–N(4)	0.4	0.1	72.1	9.5	0.5
	C(2)–C(3)–N(4)–C(5)	2.6	0.5	1.9	22.7	0.8
	C(3)–N(4)–C(5)–C(6)	33.1	7.4	0.2	33.8	4.0

[a] Numbering of the atoms is indicated in Fig. 1.

Table 2
Relative ground state energies (cm^{-1}) of SA tautomers[a]

	Enol	*Cis*-keto I	*Cis*-keto II	*Cis*-keto III	*Trans*-keto
B3LYP/6-31G** (this work)	0	1598	1596	8466	5520
HF/6-31G** (this work)	0	3063	3063	9265	5522
HF/6-31G* [11]	0		2525		5020
AM1 [8][b]	0	1400	6124	1400	2554

[a] Relative energies from the enol form. Energies are zero-point energy (ZPE) corrected values.

[b] *Cis*-keto II and *cis*-keto III are referred as *trans*-zwitterionic and *cis*-zwitterionic tautomers, respectively.

three stable tautomers exist for the *cis*-keto form. *Cis*-keto I tautomer is planar, while *cis*-keto II and *cis*-keto III tautomers are nonplanar. *Cis*-keto I and *cis*-keto III tautomers are obtained by HF/6-31G* calculations but *cis*-keto II tautomer has not been reported [11]. Semiempirical AM1 calculation provided three *cis* tautomers corresponding to the present calculations; *cis*-keto II is referred as *trans* zwitterionic in Ref. [8]. Relative ground state energies significantly depend on the calculation method as compared in Table 2. The energy of *cis*-keto II (17.5 kcal/mol) is much higher than that (4.0 kcal/mol) of *cis*-keto I by AM1 method [8], but the energies of *cis*-keto I and *cis*-keto II calculated with the B3LYP/6-31G** and HF/6-31G** basis sets are very similar or the same at the B3LYP/6-31G** level, while that of *cis*-keto III is much higher than the other two *cis*-keto tautomers.

The calculated *cis*-keto tautomers could be correlated to anomaly Stokes-shifted fluorescence. Barbara et al. [6] concluded that two *cis*-keto conformers QA* and QB* exist in the exited state by observing different two decay components in various solutions. QB* rapidly converts to QA* by vibrational relaxation, and both QA* and QB* emit fluorescence to a single ground state of a *cis*-keto tautomer. Higelin and Sixl [1] proposed that QA and QB have different conformations, and the corresponding exited-state species, QA* and QB*, provide fluorescence into QA and QB. In the dispersed fluorescence spectra of SA in a free jet, two intensity maxima are observed and the separation of the two maxima is small (700–1000 cm^{-1}). DFT and ab initio calculations show that the energy of *cis*-keto III conformer is much higher than the other two *cis*-keto conformers. The ESIPT reaction may generate a planar conformer, which is likely to be the excited electronic S_1 $(\pi\pi^*)$ state of planar *cis*-keto I conformer. Vibrationally hot *cis*-keto I in the S_1 state may easily convert to the S_1 state of nonplanar *cis*-keto II, since the *cis*-keto I may have enough vibrational energy. Thus, both *cis*-keto I and *cis*-keto II tautomers are possible candidates for the fluorescent species. *Trans*-keto tautomer is predicted to be produced via twisted S_1 $(n\pi^*)$ state of the keto form [11]. The conformation of *cis*-keto II tautomer may be more similar to that of the twisted S_1 $(n\pi^*)$ state than the conformation of *cis*-keto I tautomer. Therefore, the excited-state *cis*-keto II is predicted to be a precursor of *trans*-keto tautomer. The investigation of potential energy surfaces for *cis*-keto I, *cis*-keto II, and *trans*-keto tautomers is important to clarify the intermediate state for the formation of the photochromic transients.

The long-lived transient observed in acetonitrile solution could be ascribed to *trans*-keto tautomer. The corresponding tautomer has not been detected in the isolated state. This suggests that the populations of the long-lived transient in the lower vibrational levels of the S_1 state are much smaller in the isolated state as compared to those in solution. Rapid vibrational relaxation may play a crucial role to produce lower vibronic levels of *trans*-keto tautomer.

5. Conclusion

We have measured the LIF and dispersed fluorescence spectra of jet-cooled SA for the first time. The S_1–S_0 $(\pi\pi^*)$ transition energy is less than $24{,}800\,\mathrm{cm}^{-1}$, and the S_1 $(n\pi^*)$ state is suggested to be located below the S_1 $(\pi\pi^*)$ state at twisted conformation of SA. The broad feature of the LIF spectrum has been ascribed to overlapping of low-frequency torsional vibrations broadened by the rapid fast nonradiative processes as well as the ESIPT reactions. Three *cis*-keto tautomers are obtained by DFT and ab initio calculations. Among them the energies of two *cis*-keto tautomer are very similar. The absence of vibrational relaxation in the isolated state changes the tautomerization processes of the keto form. The long-lived transients observed in the condensed phase are not observed in the isolated state.

Acknowledgements

This work was supported in part by Grant-in-Aid for Scientific Research No. 1440177 from the Japanese Ministry of Education, Science, Sports and Culture.

References

[1] D. Higelin, H. Sixl, Chem. Phys. 77 (1983) 391.

[2] K. Kownacki, L. Kaczmarek, A. Grabowska, Chem. Phys. Lett. 210 (1993) 373.

[3] K. Kownacki, A. Mordzinski, R. Wibrandt, A. Grabowska, Chem. Phys. Lett. 227 (1994) 270.

[4] A. Grabowska, K. Kownacki, J. Karpiuk, S. Dobrin, L. Kaczmarek, Chem. Phys. Lett. 267 (1997) 132.

[5] M.I. Knyazhansky, A.V. Metelitsa, A.J. Bushkov, S.M. Aldoshin, J. Photochem. Photobiol. A 97 (1996) 121.

[6] M.I.P.F. Barbara, A.V.P.M. Renzepis, A.J.L.E. Brus, J. Am. Chem. Soc. 102 (1980) 2786.

[7] S. Mitra, N. Tamai, Chem. Phys. Lett. 282 (1998) 391.

[8] S. Mitra, N. Tamai, Chem. Phys. 246 (1999) 463.

[9] T. Yuzawa, H. Takahashi, H. Hamaguchi, Chem. Phys. Lett. 202 (1993) 221.

[10] M.E. Kletskii, A.A. Millov, A.V. Metelitsa, M.I. Knyazhansky, J. Photochem. Photobiol. A 110 (1997) 267.

[11] M.Z. Zgierski, A.A.A. Grabowska, J. Chem. Phys. 112 (2000) 6329.

[12] J. Harada, H. Uekusa, Y. Ohashi, J. Am. Chem. Soc. 121 (1999) 5809.

[13] A. Douhal, F. Lahmani, A. Zewail, Chem. Phys. 207 (1996) 477.

[14] M.D. Cohen, G.M.J. Schmidt, J. Chem. Phys. 66 (1962) 2442.

[15] T. Kawato, H. Koyama, H. Kanatomi, M. Isshiki, J. Photochem. 28 (1985) 103.

[16] T. Kawato, H. Koyama, H. Kanatomi, H. Tagawa, K. Iga, J. Photochem. Photobiol. A 78 (1994) 71.

[17] K. Nishi, H. Sekiya, H. Kawakami, A. Mori, Y. Nishimura, J. Chem. Phys. 109 (1998) 1589.

[18] H. Hamabe, T. Fukuchi, S. Shiraishi, K. Nishi, Y. Nishimura, T. Tsuji, N. Nishi, H. Sekiya, J. Phys. Chem. A 102 (1998) 3880.

[19] S. Scheiner, J. Phys. Chem. A 104 (2000) 5898.

[20] R. Destro, Acta Crystallogr. Sect. B 34 (1978) 2867.

[21] M.J. Frisch, G.W. Trucks, H.B. Schlegel, G.E. Scuseria, M.A. Robb, J.R. Cheeseman, V.G. Zakrzewski, J.A. Montgomery Jr., R.E. Stratmann, J.C. Burant, S. Dapprich, J.M. Millam, A.D. Daniels, K.N. Kudin, M.C. Strain, O. Farkas, J. Tomasi, V. Barone, M. Cossi, R. Cammi, B. Mennucci, C. Pomelli, C. Adamo, S. Clifford, J. Ochterski, G.A. Petersson, P.Y. Ayala, Q. Cui, K. Morokuma, D.K. Malick, A.D. Rabuck, K. Raghavachari, J.B. Foresman, J. Cioslowski, J.V. Ortis, A.G. Baboul, B.B. Stefanov, G. Liu, A. Liashenko, P. Piskorz, I. Komaromi, R. Gomperts, R.L. Martin, D.J. Fox, T. Keith, M.A. Al-Laham, C.Y. Peng, A. Nanayakkara, C. Gonzalez, M. Challacombe, P.M.W. Gill, B. Johnson, W. Chen, M.W. Wong, J.L. Andres, C. Gonzalez, M. Head-Gordon, E.S. Replogle, J.A. Pople, GAUSSIAN'98, Revision A.7, Gaussian, Inc., Pittsburgh, PA, 1998.

[22] M.W. Schmidt, K.K. Baldridge, J.A. Boatz, S.T. Elbert, M.S. Gordon, J.H. Jensen, S. Koseki, N. Matsunaga, K.A. Neugen, S. Su, T.L. Windus, M. Dupuis, J.A. Montgomery, J. Comput. Chem. 14 (1993) 1347.